New positive-parity bands in ^{110}Ag and systematic studies in silver isotopes

H. C. Zhang (张会成),[1] K. Y. Ma (马克岩),[1,2,3,*] J. X. Teng (滕佳欣),[1] Z. H. Zhao (赵子豪),[1] H. Wang (王豪),[1] S. Y. Liu (刘斯颖),[1] Y. C. Hao (郝宜春),[1] J. B. Lu (陆景彬),[1,†] Y. J. Ma (马英君),[1] D. Yang (杨东),[1] X. G. Wu (吴晓光),[4] Y. Zheng (郑云),[4] and C. B. Li (李聪博)[4]

[1]*College of Physics, Jilin University, Changchun 130012, China*
[2]*Chongqing Research Institute, Jilin University, Chongqing 401120, China*
[3]*Yibin Research Institute, Jilin University, Sichuan 644000, China*
[4]*China Institute of Atomic Energy, Beijing 102413, China*

(Received 23 April 2023; revised 4 July 2023; accepted 11 August 2023; published 18 August 2023)

Level structures of ^{110}Ag were studied by in-beam γ-ray spectroscopic techniques using the ^{7}Li + ^{110}Pd reaction at a beam energy of 46 MeV. Two new positive-parity rotational bands were observed, and were assigned to the $\pi g_{9/2} \otimes \nu d_{5/2}$, and $\pi g_{9/2} \otimes \nu d_{3/2}$ configurations based on the particle-rotor model and geometrical model calculations. Furthermore, the systematic studies of the $B(M1)/B(E2)$ ratios and signature splitting for the positive-parity $\pi g_{9/2} \otimes \nu g_{7/2}$ bands in odd-odd nuclei ^{106,108,110}Ag and positive-parity $\pi g_{9/2}$ bands in odd-A nuclei ^{105,107,109}Ag were performed, and it was found that these bands systematically show enhanced $B(M1)/B(E2)$ ratios at the band crossing regions and different behaviors of signature splitting before and after the backbends. In addition, the signature inversion is also observed in odd-odd and odd-A silver isotopes.

DOI: 10.1103/PhysRevC.108.024314

I. INTRODUCTION

Nuclei in the $A \approx 110$ mass region with $Z \approx 50$ have been the focus of many experimental and theoretical investigations over the past decades. In this region, a lot of interesting nuclear structure phenomena have been observed, such as magnetic rotation [1], antimagnetic rotation [2], chirality [3,4], etc. Magnetic rotation is a novel nuclear rotation occurring in weakly deformed or nearly spherical nuclei. Magnetic rotational bands observed experimentally are characterized by the strong $M1$ and very weak $E2$ transitions [5–7]. The explanation of such bands was given in terms of the shears mechanism by Frauendorf [8]. Most of the magnetic rotational bands have been already studied in Ag [9–16], Cd [1,17–22], and In [23–30] isotopes in the $A \approx 110$ mass region. Antimagnetic rotation is an exotic subject and can be explained by the two-shears-like mechanism [6]. The phenomenon of antimagnetic rotation is characterized by weak $E2$ transitions and decreasing the $B(E2)$ values with increasing spin [6]. Experimentally, the antimagnetic rotational bands in this region have mainly been reported in Pd [31–36], Cd [2,37–42], and In [24,29,43,44] isotopes. Chirality is a well-known phenomenon attracting significant attention and intensive discussion in atomic nuclei. In 1997, Frauendorf and Meng pointed out that chirality may occur in the rotating triaxial nucleus [3]. Many chiral doublet bands have been observed in the Ru [45,46], Rh [4,47–51] and Ag [11,52–55] isotopes in the $A \approx 110$ mass region. Among them, the chiral doublet bands in ^{106}Ag [53] and ^{110}Ag [55] are based on the four-quasiparticle $\pi g_{9/2} \otimes \nu h_{11/2}(g_{7/2}/d_{5/2})^2$ configuration, differing from the $\pi g_{9/2} \otimes \nu h_{11/2}$ configuration in ^{104}Rh [4], ^{106}Rh [51], and ^{104}Ag [11]. In addition, the previous studies of ^{110}Ag are mainly focused on the negative-parity bands [56,57], and the positive-parity structures are comparatively scarce [16,55]. Therefore, it is also necessary to search for new positive-parity structures in the ^{110}Ag nucleus. Moreover, systematic studies in silver isotopes are also discussed in the present work.

II. EXPERIMENTAL DETAILS

The excited states of ^{110}Ag were populated by the ^{7}Li + ^{110}Pd reaction. ^{7}Li was used to be a beam of this experiment and accelerated to an energy of 46 MeV using the HI-13 tandem accelerator, which is located at China Institute of Atomic Energy (CIAE). The target of this reaction consisted of 2.2 mg/cm^2 thick isotopically enriched ^{110}Pd metallic foil which is supported by 1.6 mg/cm^2 of Au. For the ^{7}Li + ^{110}Pd system, the main residual nuclei for the complete fusion are ^{112}In and ^{113}In. ^{7}Li is a weakly bound nucleus, therefore incomplete fusion can occur in this reaction [58–61]. ^{7}Li can break into ^{3}H and ^{4}He during the reaction, in which the main residual nuclei for the incomplete fusion of the ^{4}He fragment are ^{111}Cd($3n$) and ^{112}Cd($2n$), and for the ^{3}H fragment they are ^{109}Ag($4n$) and ^{110}Ag($3n$). In the present experiment, the most dominant reaction mechanism producing ^{110}Ag is from the incomplete fusion reaction. A total of approximately 1.7×10^8 γ-γ events were accumulated by nine Compton-suppressed high-purity germanium (HPGe) detectors, two planar-type HPGe detectors, and one clover detector. In the array, these

*mky@jlu.edu.cn
†ljb@jlu.edu.cn

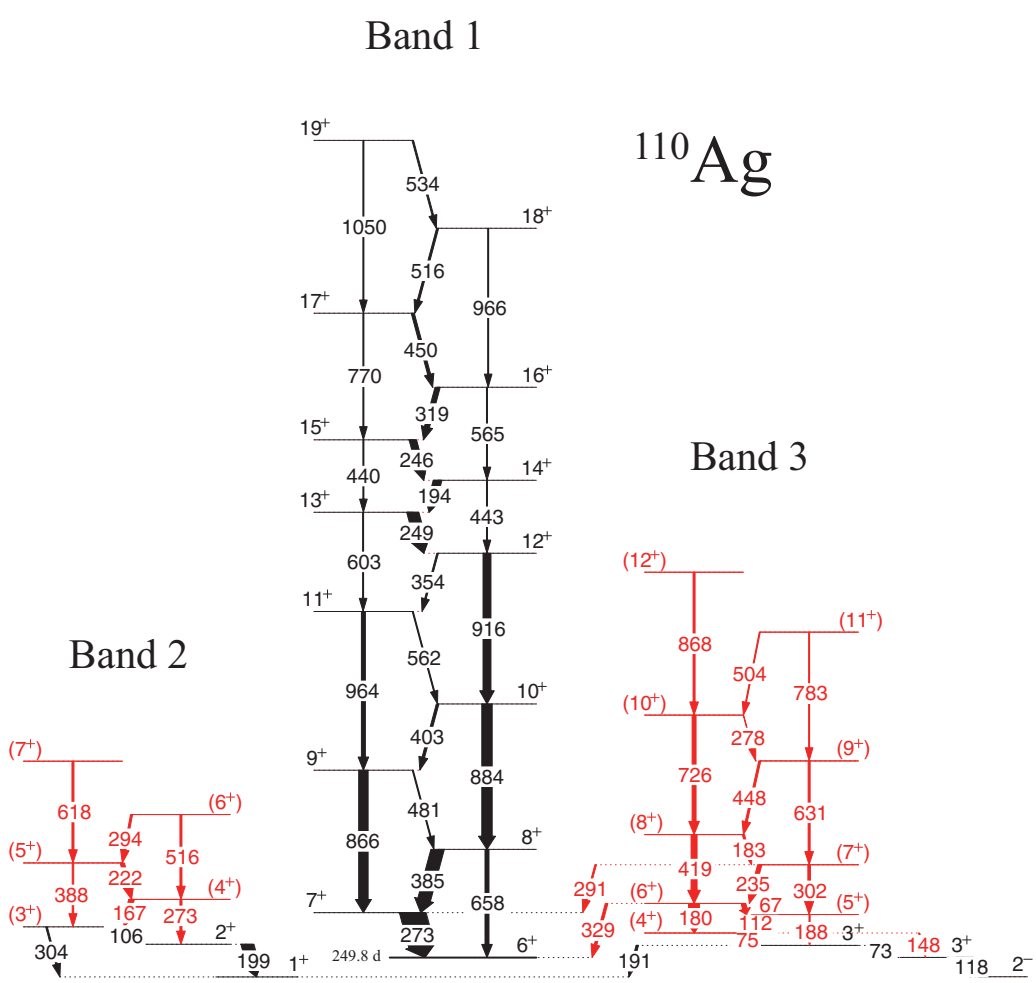

FIG. 1. Partial level scheme of ^{110}Ag deduced from the present work. Transition energies are given in keV and their measured relative intensities are proportional to the widths of the arrows. New transitions and levels are marked as red. The lifetime for the 6^+ isomer in band 1 is taken from the previous work [63].

detectors were arranged at forward (40°), 90°, and backward (140°) directions with respect to the beam direction. In the offline analysis, energy and efficiency calibrations of these detectors were carried out by using ^{133}Ba and ^{152}Eu as the standard sources. In order to extract the coincidence relationships with γ rays and the multipolarities of the transitions, the data were sorted into a fully symmetrized γ-γ coincidence matrix and an asymmetric directional correlation ratios of oriented states (DCO) matrix [62]. The two asymmetric DCO matrices were created by sorting the detectors at ±40° on one axis and the other axis corresponding to the 90° detectors. In the present geometry, the DCO ratios which were extracted from pure dipole and quadrupole transitions were found to be about 0.6(1.0) and 1.0(1.7), respectively, by gating on the stretched quadrupole (dipole) transitions. The present work is from the same data set as that in Ref. [55].

III. RESULTS

The partial level scheme of ^{110}Ag deduced from the current work and typical gated γ-ray coincidence spectra are shown in Figs. 1 and 2, respectively. Nearly 30 new transitions are added to the level scheme of ^{110}Ag. As shown in Fig. 1, band 1 has been reported in the previous work [16,55] and two new rotational bands labeled 2 and 3 were observed in the current work. The γ-ray energies, relative intensities, DCO ratios and spin-parity assignments are listed in Table. I. The relevant details of the level scheme will be described below.

The positive-parity band 1 of ^{110}Ag was reported in the previous work [16]. Subsequently, this band was further confirmed by Ma [55]. Band 2 is a newly observed rotational band built on the previously known $I^\pi = 2^+$ state [64], and decays to the ground state $I^\pi = 1^+$ via two linking transitions with energies of 199 and 304 keV [65]. Figure 2(a) shows the spectrum gated by the 106 keV γ transition. Multipolarity analysis indicates that 273, 388, 516, and 618 keV intraband transitions are of $\Delta I = 2$ character, and 167, 222, and 294 keV transitions are of $\Delta I = 1$ character. Thus, band 2 is suggested as a positive-parity band, and the spin and parity of this band are pushed up to $I^\pi = (7^+)$.

Band 3, consisting of eight magnetic dipole ($M1$) transitions and eight electric quadruple ($E2$) transitions, was

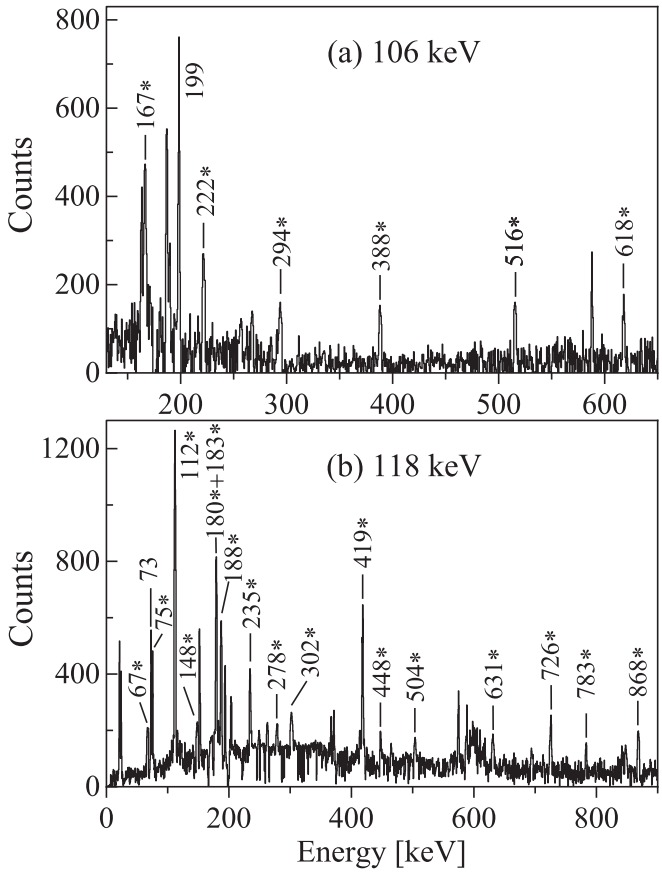

FIG. 2. γ-ray coincidence spectra with gates set on the (a) 106 keV and (b) 118 keV transitions. The newly identified γ rays are marked with asterisks.

observed for the first time. It is built on the previously known positive $I^\pi = 3^+$ level [65] and extended up to the $I^\pi = (12^+)$ state in the current work. Multipolarity analysis indicates that the 112, 235, 183, 448, and 504 keV intraband transitions are of $\Delta I = 1$ character and the 180, 188, 302, 419, 631, 726, and 868 keV intraband transitions are of $\Delta I = 2$ character. The observations of the new $E2$ crossover transitions can confirm the ordering of the dipole transitions of band 3 up to the $I^\pi = (11^+)$ level. In addition, two new 291 and 329 keV linking transitions between band 1 and band 3 were observed, further supporting the excitation energies of band 3. A typical spectrum generated from the gate on 118 keV transition is shown in Fig. 2(b).

TABLE I. Energies, intensities, and DCO ratios, initial and final state spins, and multipolarities for transitions assigned to ^{110}Ag in the present experiment. The data for band 1 obtained from the same experiment were already reported in Ref. [55].

E_γ[a] (keV)	I_γ[b]	R_{DCO}[c]	R_{DCO}[d]	I_i^π–I_f^π	Multipolarity
Band 2					
105.9	15(4)	0.7(3)	0.9(2)	$(3^+) \to 2^+$	$M1$
166.7	10(3)		0.8(3)	$(4^+) \to (3^+)$	$(M1/E2)$
221.6	8(3)		0.7(3)	$(5^+) \to (4^+)$	$(M1/E2)$
272.6	4(2)		1.7(9)	$(4^+) \to 2^+$	$(E2)$
294.1	4(2)		0.8(4)	$(6^+) \to (5^+)$	$(M1/E2)$
388.2	3(2)		1.5(9)	$(5^+) \to (3^+)$	$(E2)$
515.7	4(2)		1.8(8)	$(6^+) \to (4^+)$	$(E2)$
618.2	4(3)		1.6(7)	$(7^+) \to (5^+)$	$(E2)$
Band 3					
67.3	4(2)			$(6^+) \to (5^+)$	$(M1/E2)$
75.3	5(2)			$(4^+) \to 3^+$	$(M1/E2)$
112.2	23(5)	0.5(1)	1.1(2)	$(5^+) \to (4^+)$	$(M1/E2)$
179.6	19(5)	0.8(2)		$(6^+) \to (4^+)$	$(E2)$
183.3	4(2)		0.9(5)	$(8^+) \to (7^+)$	$(M1/E2)$
187.7	12(3)		1.6(5)	$(5^+) \to 3^+$	$(E2)$
235.2	8(3)		1.2(4)	$(7^+) \to (6^+)$	$(M1/E2)$
278.4	<2			$(10^+) \to (9^+)$	$(M1/E2)$
302.4	5(2)		1.5(8)	$(7^+) \to (5^+)$	$(E2)$
418.8	12(4)		1.8(6)	$(8^+) \to (6^+)$	$(E2)$
447.6	4(2)		0.8(4)	$(9^+) \to (8^+)$	$(M1/E2)$
504.2	3(2)		0.6(3)	$(11^+) \to (10^+)$	$(M1/E2)$
630.8	4(2)		1.5(9)	$(9^+) \to (7^+)$	$(E2)$
725.6	8(3)	0.9(3)	1.7(6)	$(10^+) \to (8^+)$	$(E2)$
782.9	<2			$(11^+) \to (9^+)$	$(E2)$
868.2	4(2)	0.8(4)		$(12^+) \to (10^+)$	$(E2)$
Linking transitions					
73.1	6(2)			$3^+ \to 3^+$	$M1$
117.5	34(6)	0.5(1)	1.1(2)	$3^+ \to 2^-$	$E1$
148.5	<2			$(4^+) \to 3^+$	$(M1/E2)$
191.4	4(2)		1.6(8)	$3^+ \to 1^+$	$(E2)$
198.5	24(6)		0.9(2)	$2^+ \to 1^+$	$M1$
291.3	3(2)	0.9(5)		$(7^+) \to 7^+$	$(M1/E2)$
304.2	3(2)		1.8(9)	$(3^+) \to 1^+$	$(E2)$
329.3	5(3)	0.9(4)		$(6^+) \to 6^+$	$(M1/E2)$

[a]The energy uncertainty is about 0.2 keV for strong transitions and about 0.5 keV for weak transitions.
[b]Intensities are corrected for detector efficiency and normalized to 100 for the same 191.5 keV transition as in Ref. [55], but the 191.5 keV transition is not shown in Fig. 1.
[c]DCO ratios from a gate on the quadrupole transition.
[d]DCO ratios from a gate on the dipole transition.

IV. DISCUSSION

Band 1 built on the $I^\pi = 6^+$ isomer was studied in Refs. [16,55]. A similar structure in neighboring ^{108}Ag nucleus with the $\pi g_{9/2} \otimes \nu g_{7/2}$ configuration was also reported in the previous study [66]. For comparison, the experimental angular momentum (i_x) as a function of frequency for band 1 in ^{110}Ag and that of band 2 in ^{108}Ag is plotted in Fig. 3(a). It is clear from Fig. 3(a) that the two bands show similar behaviors, including the frequencies of the observed alignment ($\hbar\omega \approx 0.3$ MeV) and large alignment gain of $\approx 8\hbar$. As is well known, the sharp backbends come from an aligned pair of $h_{11/2}$ neutrons in the the $A \approx 110$ mass region [67]. It indicates that band 1 of ^{110}Ag also has the same configuration as that of band 2 in ^{108}Ag [66], where band 2 has been assigned to the $\pi g_{9/2} \otimes \nu g_{7/2}$ configuration. Hence, the configuration for band 1 in ^{110}Ag is tentatively suggested as $\pi g_{9/2} \otimes \nu g_{7/2}$ configuration before the backbend, and $\pi g_{9/2} \otimes \nu g_{7/2} h_{11/2}^2$ after the backbend. Additionally, the configuration assignment for band 1 of ^{110}Ag is also supported by the fact that the

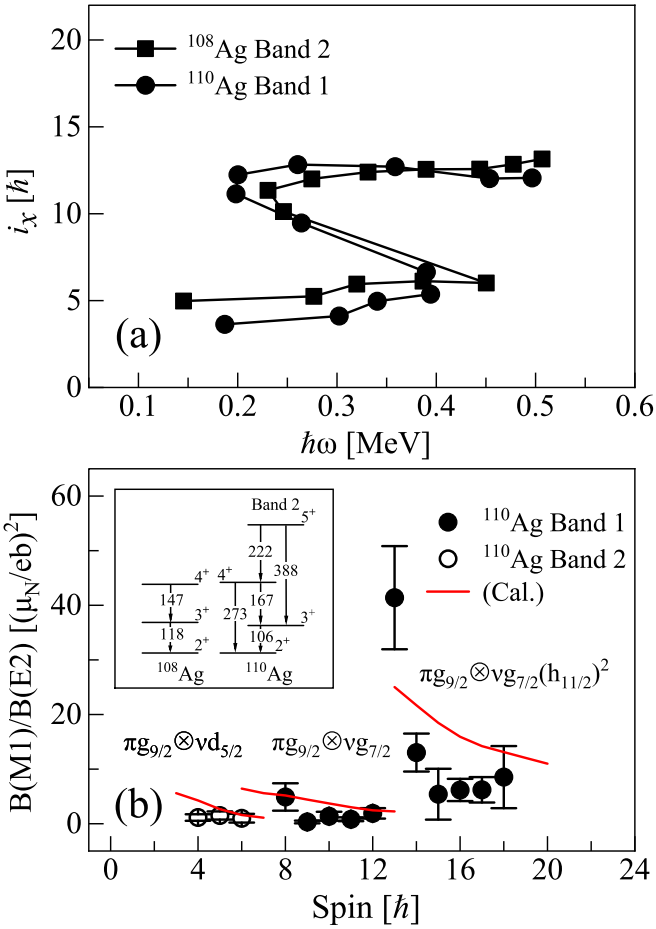

FIG. 3. (a) Aligned angular momenta as a function of rotational frequency for band 1 in ^{110}Ag and the similar band 2 in ^{108}Ag. (b) The experimental and predicted $B(M1)/B(E2)$ ratios as a function of spin for bands 1 and 2 in ^{110}Ag [55]. The inset presents the partial level scheme of band 2 in ^{110}Ag and the similar structure in ^{108}Ag. Harris parameters are $J_0 = 3.6\,\mathrm{MeV}^{-1}\hbar^2$ and $J_1 = 29.8\,\mathrm{MeV}^{-3}\hbar^4$ for ^{108}Ag and ^{110}Ag.

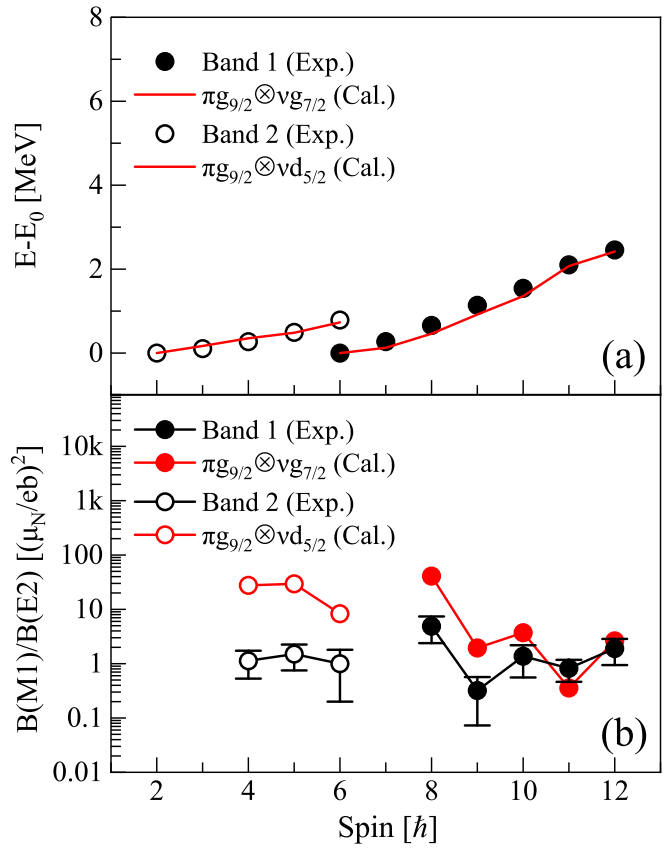

FIG. 4. (a) The experimental excitation energies $E(I)$ and (b) $B(M1)/B(E2)$ for bands 1 and 2 in ^{110}Ag in comparison with the calculated results by the PRM. The $\pi g_{9/2} \otimes \nu g_{7/2}$ (for band 1) and $\pi g_{9/2} \otimes \nu d_{5/2}$ (for band 2) configurations with the deformation parameters $(\beta, \gamma) = (0.2, 46.8^\circ)$ were adopted in the calculations.

predicted $B(M1)/B(E2)$ ratios of the geometrical model [68] are in good agreement with the experimental values before and after the band crossing, as shown in Fig. 3(b).

Band 2 is a new band and the spin is up to $I^\pi = (7^+)$ in the present work. Considering the Fermi surface for both protons and neutrons of ^{110}Ag, it is evident that only the $g_{9/2}$ Nilsson orbital lies near the Fermi surface for the proton, while near the neutron Fermi surface the Nilsson orbitals are the $g_{7/2}$, $d_{5/2}$, $d_{3/2}$, and $h_{11/2}$ orbitals in this mass region. The $g_{9/2}$ proton and $h_{11/2}$ neutron can only make up the negative-parity band. $g_{7/2}$ and $d_{5/2}$ are the candidates for the neutron orbitals of band 2, forming the positive parity and the initial 2^+ state. However, the $g_{7/2}$ orbital is occupied by band 1. Thus, band 2 is tentatively assigned as the $\pi g_{9/2} \otimes \nu d_{5/2}$ configuration. Indeed, a similar structure has also been observed in neighboring ^{108}Ag nucleus [69]. For comparison, the partial level scheme of band 2 in ^{110}Ag and that of the similar structure in ^{108}Ag are shown in the inset of Fig. 3(b). One can see from the inset of Fig. 3(b) that the decay pattern and the excitation energies of two structures are very similar. It indicates that two such nuclei may have a common origin, and the structure in ^{108}Ag has previously been proposed as $\pi g_{9/2} \otimes \nu d_{5/2}$ configuration. Hence, it is probable that band 2 of ^{110}Ag has the same configuration as that in ^{108}Ag. As shown in Fig. 3(b), the predicted $B(M1)/B(E2)$ ratios of the $\pi g_{9/2} \otimes \nu d_{5/2}$ configuration generally agree with the experimental values in band 2, providing extra evidence for the configuration assignment for band 2 in ^{110}Ag.

To further investigate the features for bands 1 and 2, calculations based on the particle-rotor model (PRM) [70–73] were performed. In the present work, $E(I)$ and $B(M1)/B(E2)$ calculated by the PRM for bands 1 and 2 with the $\pi g_{9/2} \otimes \nu g_{7/2}$ and $\pi g_{9/2} \otimes \nu d_{5/2}$ configurations are presented in Figs. 4(a) and 4(b), in comparison with the experimental data. In Fig. 4(a), the calculated $E(I)$ for bands 1 and 2 reproduce the variation trend of excitation energies observed experimentally. The deviation between the predicted $B(M1)/B(E2)$ ratios and the experiment in Fig. 4(b) might be attributed to the fact that the present PRM does not consider the mixture of configurations [74,75], i.e., the mixture of $d_{5/2}$ and $g_{7/2}$ orbitals is neglected in the PRM calculations.

Positive-parity band 3 is reported for the first time in the present study. Previously, the positive-parity $g_{7/2}$ and $d_{5/2}$

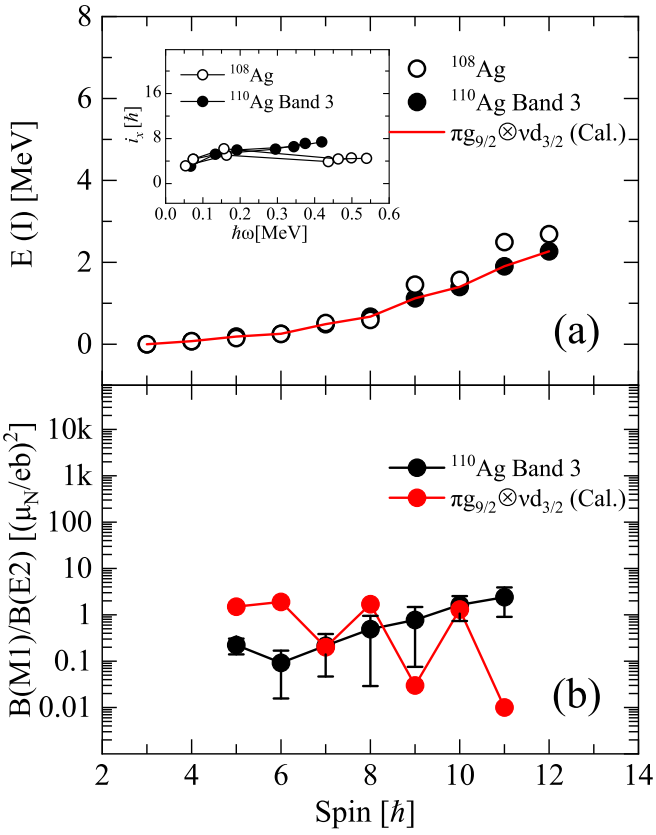

FIG. 5. (a) The comparison of the excitation energies $E(I)$ of band 3 in ^{110}Ag, the similar structure in ^{108}Ag [66,76,77], and the calculated results by the PRM as a function of spin. (b) The comparison of the experimental $B(M1)/B(E2)$ for band 3 in comparison with the calculated results by the PRM. The $\pi g_{9/2} \otimes \nu d_{3/2}$ configuration (for band 3) with the deformation parameters $(\beta, \gamma) = (0.2, 42.5^\circ)$ were adopted in the calculations. The inset presents a comparison of the experimental alignment for band 3 in ^{110}Ag and the similar structure in ^{108}Ag as a function of rotational frequency. Harris parameters are $J_0 = 3.6\ \mathrm{MeV}^{-1}\hbar^2$, $J_1 = 29.8\ \mathrm{MeV}^{-3}\hbar^4$ for ^{108}Ag and ^{110}Ag.

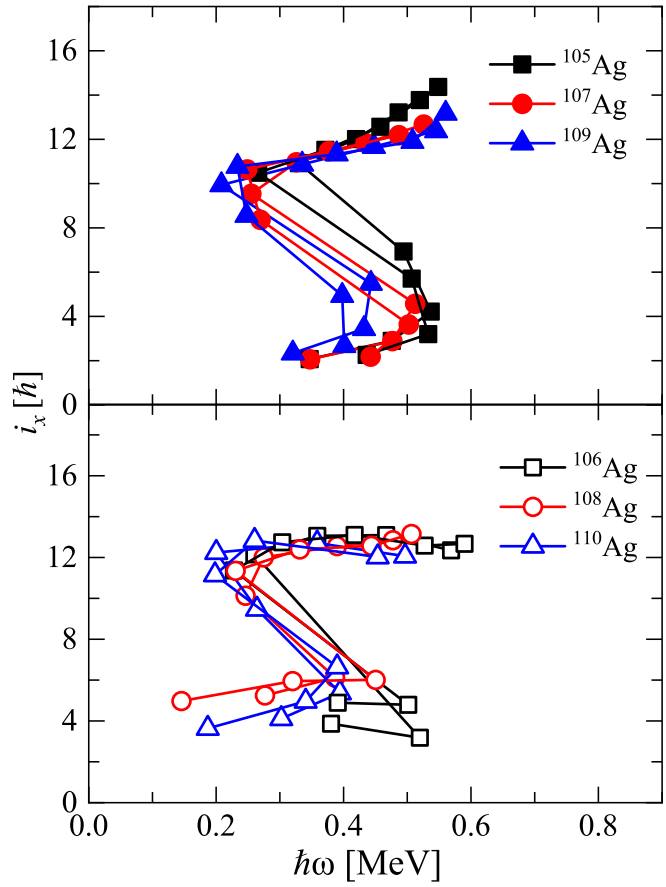

FIG. 6. Experimental alignment plots for the bands with the $\pi g_{9/2} \otimes \nu g_{7/2}$ configuration in ^{106,108,110}Ag [55,66,78] and the bands built on the $\pi g_{9/2}$ configuration in ^{105,107,109}Ag [52,79,80]. Harris parameters are $J_0 = 3.6\ \mathrm{MeV}^{-1}\hbar^2$, $J_1 = 29.8\ \mathrm{MeV}^{-3}\hbar^4$ for ^{106,108,110}Ag and $J_0 = 7\ \mathrm{MeV}^{-1}\hbar^2$, $J_1 = 9\ \mathrm{MeV}^{-3}\hbar^4$ for ^{105,107,109}Ag.

orbitals have been assigned to bands 1 and 2, respectively. Thus, band 3 is tentatively adopted as the $\pi g_{9/2} \otimes \nu d_{3/2}$ configuration. Moreover, a similar structure has also been observed in neighboring ^{108}Ag [76,77]. For comparison, the excitation energies of band 3 in ^{110}Ag and those of similar structure in ^{108}Ag are extracted and presented in Fig. 5(a). It can be seen that the trend and amplitude of the energy separation between the same spins are close in ^{108}Ag and ^{110}Ag. Besides, (i_x) for these two structures is plotted in the inset in Fig. 5(a). As seen in the inset, the pattern of (i_x) for the two structures is similar. The similarity of the alignments of ^{108}Ag and ^{110}Ag provides additional support for the $\pi g_{9/2} \otimes \nu d_{3/2}$ configuration assignment of band 3 in ^{110}Ag. In addition, the calculated $E(I)$ and $B(M1)/B(E2)$ ratios are presented in Figs. 5(a) and 5(b) in comparison with the experimental data of band 3 in ^{110}Ag. As illustrated in Fig. 5(a), the experimental $E(I)$ is reproduced by the present PRM calculation. And the magnitude of the calculated $B(M1)/B(E2)$ ratios in Fig. 5(b) is generally in agreement with the experimental data.

Furthermore, systematic studies of the bands with $\pi g_{9/2} \otimes \nu g_{7/2}$ configuration in odd-odd nuclei ^{106,108,110}Ag [55,66,78] and those with $\pi g_{9/2}$ configuration in odd-A nuclei ^{105,107,109}Ag [52,79,80] are also discussed in the present work. The experimental alignment of these bands is plotted in Fig. 6. As shown in Fig. 6, all of these bands exhibit sharp backbends with large alignment gain of $\approx 8\hbar$ occurring at a frequency of about 0.3 MeV. The large gain in aligned angular momentum is associated with the alignment of the $h_{11/2}$ neutrons, which is consistent with the predicted quasineutron alignment [67]. Meanwhile, the experimental $B(M1)/B(E2)$ ratios of these bands have been plotted in Fig. 7, where the $B(M1)/B(E2)$ ratios suddenly increase a lot near $I^\pi = 13^+$ in odd-odd nuclei ^{106,108,110}Ag and $I^\pi = 25/2^+$ in odd-A nuclei ^{105,107,109}Ag. Coincidentally, the backbends of these bands, which are attributed to the two aligned $h_{11/2}$ neutrons in the $A \approx 110$ mass region [81], also occur near $I^\pi = 13^+$ and $I^\pi = 25/2^+$ in odd-odd and odd-A Ag isotopes. Hence, it is speculated that the suddenly enhanced $B(M1)/B(E2)$ ratios may be related to the pair of aligned $h_{11/2}$ neutrons. In ^{109}Ag, this phenomenon is interpreted to be due to a change in the rotational axis [80]. It

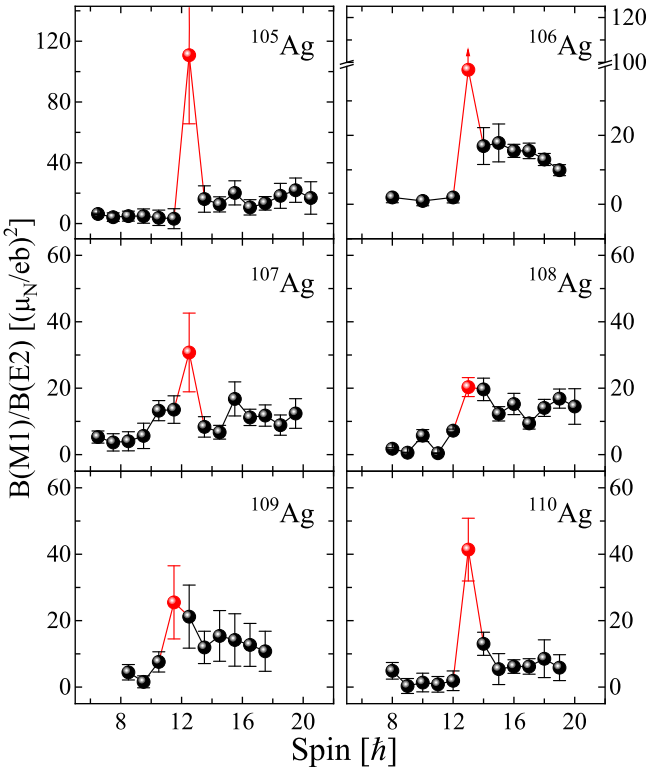

FIG. 7. The experimental $B(M1)/B(E2)$ ratios as a function of spin for the bands built on the $\pi g_{9/2} \otimes \nu g_{7/2}$ configuration in ^{106,108,110}Ag [55,66,78] and the bands built on the $\pi g_{9/2}$ configuration in ^{105,107,109}Ag [52,79,80].

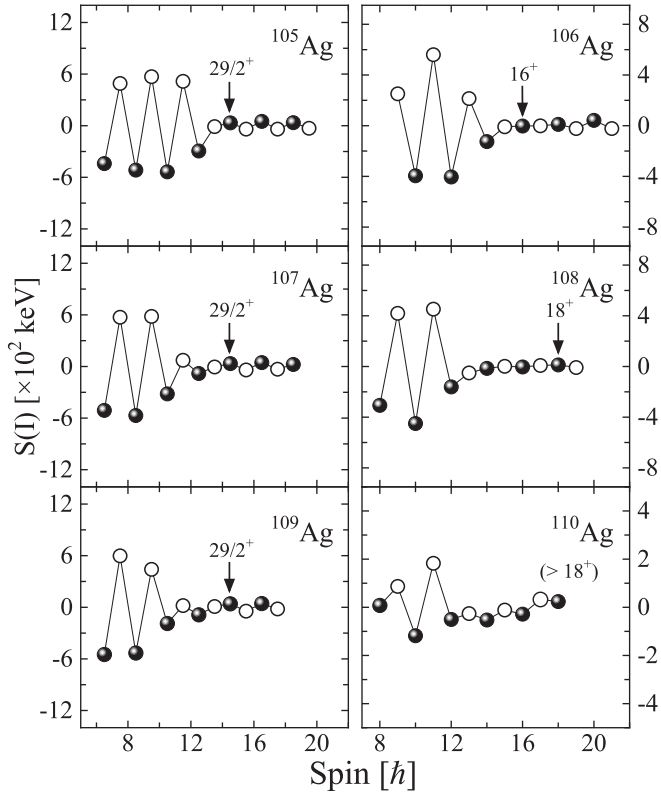

FIG. 8. The energy staggering parameter $S(I) = E(I) - E(I-1) - [E(I+1) - E(I) + E(I-1) - E(I-2)]/2$ as a function of spin for the bands built on the $\pi g_{9/2} \otimes \nu g_{7/2}$ configuration in ^{106,108,110}Ag and the bands built on the $\pi g_{9/2}$ configuration in ^{105,107,109}Ag. Solid and open circles correspond to favored and unfavored signatures, respectively.

is conjectured that these systematic features observed in other nuclei are also likely to be attributable to this explanation.

Moreover, it is to be noted from Fig. 1 that band 1 in ^{110}Ag before backbend (below $I^\pi = 12^+$ level) shows strong $E2$ transitions between the favored spin states, whereas band 1 after backbend (above $I^\pi = 13^+$ level) consists of strong $M1$ and weak $E2$ transitions. This observation indicates that these two structures before and after backbend are dissimilar in nature. Interestingly, this phenomenon is also observed systematically in its other neighboring odd-odd nuclei ^{106,108}Ag [66,78] and odd-A nuclei ^{105,107,109}Ag [52,79,80]. For the nuclei mentioned above, it is inferred that the corresponding bands before backbend may originate from electric rotation, while the bands after backbend might result from magnetic rotation. Indeed, the bands after backbend have been suggested as the magnetic rotational bands in ^{106,107,109,110}Ag [55,78–80]. Meanwhile, the observed $S(I)$ for the bands before the backbend shows a clear signature splitting that is the character of the electric rotation, as shown in Fig. 8. After the backbend, the curves of $S(I)$ become smooth, which is a feature of the magnetic rotation [8]. Hence, we speculate that a transition from electric rotation to magnetic rotation probably occurs in the odd-odd nuclei ^{106,108,110}Ag and odd-A nuclei ^{105,107,109}Ag.

It is worth mentioning that the very similar observations of a significant reduction in staggering after a crossing were also found in the $A \approx 150$ mass region [82], where the sudden reduction of energy staggering is interpreted to be due to changing shapes before and after the crossing [82]. In odd-odd nuclei ^{106,108,110}Ag and odd-A nuclei ^{105,107,109}Ag, the high-Ω $\pi g_{9/2}$ orbital drives the nuclei towards oblate deformation, while the first crossing results from the high-j, low-Ω $\nu h_{11/2}$ neutrons driving the nuclei towards prolate deformation. The delicate interplay of the high-Ω $\pi g_{9/2}$ and low-Ω $\nu h_{11/2}$ orbitals would influence the overall shape of the nucleus and result in γ softness. Hence, we infer that the systematic energy staggering behavior before and after the crossing observed in Ag isotopes is also likely to be related to a change in nuclear shape.

In addition, the signature inversion [83] is also observed in the odd-odd nuclei ^{106,108,110}Ag and odd-A nuclei ^{105,107,109}Ag as seen in Fig. 8, where the spin inversion is near $I^\pi = 29/2^+$ in the odd-A nuclei ^{105,107,109}Ag, while the odd-odd nuclei ^{106,108,110}Ag it seem to show an increasing trend for spin inversion with increasing neutron number. This variation trend is similar to that of the $\pi h_{11/2} \otimes \nu h_{11/2}$ bands in the $A \approx 130$ mass region [84,85].

V. SUMMARY

Excited states of the ^{110}Ag nucleus were populated by the ^{7}Li + ^{110}Pd reaction. Compared with the previous work, the

level scheme of ^{110}Ag was extended and two positive-parity rotational bands with the addition of 26 new γ rays and 13 new levels were observed. These two new bands were assigned to the $\pi g_{9/2} \otimes \nu d_{5/2}$ and $\pi g_{9/2} \otimes \nu d_{3/2}$ configurations based on the PRM and geometrical model calculations. Furthermore, the systematic studies of the $B(M1)/B(E2)$ ratios and signature splitting for the positive-parity $\pi g_{9/2} \otimes \nu g_{7/2}$ bands in odd-odd nuclei ^{106,108,110}Ag and positive-parity $\pi g_{9/2}$ bands in odd-A nuclei ^{105,107,109}Ag were performed, and the results show that the enhanced $B(M1)/B(E2)$ ratios occur systematically at the band crossing regions and different behaviors of signature splitting are found before and after the backbends. These interesting phenomena are likely to result from the evolution from electric rotation to magnetic rotation. Besides, a change in nuclei shape may also result in the occurrence of these phenomena.

ACKNOWLEDGMENTS

This work is supported by the Jilin Scientific and Technological Development Program (20230101009JC), National Natural Science Foundation of China (12175086, 11775098, U1867210, 11405072), Science and Technology Research Planning Project of Jilin Provincial Department of Education (JJKH20220965KJ), Natural Science Foundation of Chongqing, China (CSTB2022NSCQMSX0315), Natural Science Foundation of Sichuan China (23NSFSC1051), and Graduate Innovation Fund of Jilin University (101832020CX080).

[1] R. M. Clark, S. J. Asztalos, B. Busse, C. J. Chiara, M. Cromaz, M. A. Deleplanque, R. M. Diamond, P. Fallon, D. B. Fossan *et al.*, Phys. Rev. Lett. **82**, 3220 (1999).
[2] A. J. Simons, R. Wadsworth, D. G. Jenkins, R. M. Clark, M. Cromaz, M. A. Deleplanque, R. M. Diamond, P. Fallon, G. J. Lane *et al.*, Phys. Rev. Lett. **91**, 162501 (2003).
[3] S. Frauendorf and J. Meng, Nucl. Phys. A **617**, 131 (1997).
[4] C. Vaman, D. B. Fossan, T. Koike, K. Starosta, I. Y. Lee, and A. O. Macchiavelli, Phys. Rev. Lett. **92**, 032501 (2004).
[5] H. Hubel, Prog. Part. Nucl. Phys. **54**, 1 (2005).
[6] S. Frauendorf, Rev. Mod. Phys. **73**, 463 (2001).
[7] R. M. Clark and A. O. Macchiavelli, Annu. Rev. Nucl. Part. Sci. **50**, 1 (2000).
[8] S. Frauendorf, Nucl. Phys. A **557**, 259 (1993).
[9] V. Singh, S. Sihotra, S. S. Malik, G. H. Bhat, R. Palit, J. A. Sheikh, S. Kumar, N. Singh, K. Singh *et al.*, Phys. Rev. C **94**, 044320 (2016).
[10] S. Ray, N. S. Pattabiraman, Krishichayan, A. Chakraborty, S. Mukhopadhyay, S. S. Ghugre, S. N. Chintalapudi, A. K. Sinha, U. Garg, S. Zhu, B. Kharraja, and D. Almehed, Phys. Rev. C **77**, 024305 (2008).
[11] Z. G. Wang, M. L. Liu, Y. H. Zhang, X. H. Zhou, B. T. Hu, N. T. Zhang, S. Guo, B. Ding, Y. D. Fang *et al.*, Phys. Rev. C **88**, 024306 (2013).
[12] A. Y. Deo, S. B. Patel, S. K. Tandel, S. Muralithar, R. P. Singh, R. Kumar, R. K. Bhowmik, S. S. Ghugre, A. K. Singh *et al.*, Phys. Rev. C **73**, 034313 (2006).
[13] C. Y. He, L. H. Zhu, X. G. Wu, S. X. Wen, G. S. Li, Y. Liu, Z. M. Wang, X. Q. Li, X. Z. Cui *et al.*, in *Nuclear Physics and Astrophysics: From Stable Beams to Exotic Nuclei, Cappadocia, Turkey 25–30 June 2008*, edited by I. Boztosun and A. B. Balantekin, AIP Conf. Proc. No. 1072 (AIP, New York, 2008), p. 302.
[14] S. H. Yao, H. L. Ma, L. H. Zhu, X. G. Wu, C. Y. He, Y. Zheng, B. Zhang, G. S. Li, C. B. Li *et al.*, Phys. Rev. C **89**, 014327 (2014).
[15] K. Y. Ma, J. B. Lu, J. Li, Y. J. Ma, D. Yang, W. J. Sun, Q. Y. Yang, X. Guan, J. Q. Wang *et al.*, Eur. Phys. J. A **56**, 209 (2020).
[16] B. Das, P. Datta, S. Chattopadhyay, S. Roy, R. Raut, R. K. Bhowmik, A. Goswami, H. C. Jain, R. Kumar *et al.*, Phys. Rev. C **98**, 014326 (2018).
[17] J. Persson, J. Cederkall, M. Lipoglavsek, M. Palacz, A. Atac, J. Blomqvist, C. Fahlander, H. Grawe, A. Johnson *et al.*, Nucl. Phys. A **627**, 101 (1997).
[18] S. D. Robinson, S. J. Freeman, D. P. Balamuth, M. Carpenter, M. Devlin, B. G. Dong, J. L. Durell, P. Hausladen, D. R. LaFosse *et al.*, J. Phys. G **28**, 1415 (2002).
[19] D. Choudhury, R. Palit, P. Singh, J. Sethi, S. Saha, S. Biswas, H. C. Jain, V. Nanal, R. G. Pillay *et al.*, Phys. Rev. C **91**, 014318 (2015).
[20] S. Roy, P. Datta, S. Pal, S. Chattopadhyay, S. Bhattacharya, A. Goswami, H. C. Jain, P. K. Joshi, R. K. Bhowmik *et al.*, Phys. Rev. C **81**, 054311 (2010).
[21] S. Juutinen, P. Simecek, C. Fahlander, R. Julin, J. Kumpulainen, A. Lampinen, T. Lonnroth, A. Maj, S. Mitarai *et al.*, Nucl. Phys. A **577**, 727 (1994).
[22] S. Juutinen, R. Julin, M. Piiparinen, P. Ahonen, B. Cederwall, C. Fahlander, A. Lampinen, T. Lonnroth, A. Maj *et al.*, Nucl. Phys. A **573**, 306 (1994).
[23] D. Negi, T. Trivedi, A. Dhal, S. Kumar, V. Kumar, S. Roy, M. K. Raju, S. Appannababu, G. Mohanto *et al.*, Phys. Rev. C **81**, 054322 (2010).
[24] C. J. Chiara, D. B. Fossan, V. P. Janzen, T. Koike, D. R. LaFosse, G. J. Lane, S. M. Mullins, E. S. Paul, D. C. Radford *et al.*, Phys. Rev. C **64**, 054314 (2001).
[25] D. Negi, T. Trivedi, A. Dhal, S. Kumar, V. Kumar, S. Roy, M. K. Raju, S. Appannababu, G. Mohanto *et al.*, Phys. Rev. C **85**, 057301 (2012).
[26] P. Banerjee, S. Ganguly, M. K. Pradhan, H. P. Sharma, S. Muralithar, R. P. Singh, and R. K. Bhowmik, Phys. Rev. C **83**, 024316 (2011).
[27] T. Trivedi, R. Palit, J. Sethi, S. Saha, S. Kumar, Z. Naik, V. V. Parkar, B. S. Naidu, A. Y. Deo *et al.*, Phys. Rev. C **85**, 014327 (2012).
[28] S. Naguleswaran, R. S. Chakrawarthy, U. Garg, K. L. Lamkin, G. Smith, J. C. Walpe, A. Galindo-Uribarri, V. P. Janzen, D. C. Radford *et al.*, Phys. Rev. C **72**, 044304 (2005).
[29] K. Y. Ma, J. B. Lu, J. Li, D. Yang, Y. J. Ma, W. J. Sun, X. Guan, D. M. Zhang, L. H. Zhu *et al.*, Phys. Rev. C **100**, 014326 (2019).
[30] C. B. Li, J. Li, X. G. Wu, X. F. Li, Y. Zheng, C. Y. He, G. S. Li, S. H. Yao, B. B. Yu *et al.*, Nucl. Phys. A **892**, 34 (2012).
[31] S. Sihotra, Int. J. Mod. Phys. E **31**, 2250020 (2022).

[32] S. Sihotra, D. Kumar, M. Kaur, V. Singh, S. Saha, J. Sethi, R. Palit, N. Singh, and D. Mehta, Phys. Rev. C **102**, 034321 (2020).

[33] M. Sugawara, T. Hayakawa, M. Oshima, Y. Toh, A. Osa, M. Matsuda, T. Shizuma, Y. Hatsukawa, H. Kusakari *et al.*, Phys. Rev. C **92**, 024309 (2015).

[34] H. Jia, B. Qi, C. Liu, Q. Hu, and S. Y. Wang, Phys. Rev. C **97**, 024335 (2018).

[35] N. Rather, S. Roy, P. Datta, S. Chattopadhyay, A. Goswami, S. Nag, R. Palit, S. Pal, S. Saha *et al.*, Phys. Rev. C **89**, 061303(R) (2014).

[36] Y. K. Pan, K. Y. Ma, and J. B. Lu, Chin. Phys. C **46**, 094001 (2022).

[37] D. Choudhury, A. K. Jain, M. Patial, N. Gupta, P. Arumugam, A. Dhal, R. K. Sinha, L. Chaturvedi, P. K. Joshi *et al.*, Phys. Rev. C **82**, 061308(R) (2010).

[38] D. Choudhury, A. K. Jain, G. A. Kumar, S. Kumar, S. Singh, P. Singh, M. Sainath, T. Trivedi, J. Sethi *et al.*, Phys. Rev. C **87**, 034304 (2013).

[39] A. J. Simons, R. Wadsworth, D. G. Jenkins, R. M. Clark, M. Cromaz, M. A. Deleplanque, R. M. Diamond, P. Fallon, G. J. Lane *et al.*, Phys. Rev. C **72**, 024318 (2005).

[40] P. Datta, S. Chattopadhyay, S. Bhattacharya, T. K. Ghosh, A. Goswami, S. Pal, M. Saha Sarkar, H. C. Jain, P. K. Joshi *et al.*, Phys. Rev. C **71**, 041305(R) (2005).

[41] S. Roy, S. Chattopadhyay, P. Datta, S. Pal, S. Bhattacharya, R. K. Bhowmik, A. Goswami, H. C. Jain, R. Kumar *et al.*, Phys. Lett. B **694**, 322 (2011).

[42] C. Majumder, H. P. Sharma, S. Chakraborty, and S. S. Tiwary, Int. J. Mod. Phys. E **27**, 1850034 (2018).

[43] X. W. Li, J. Li, J. B. Lu, K. Y. Ma, Y. H. Wu, L. H. Zhu, C. Y. He, X. Q. Li, Y. Zheng *et al.*, Phys. Rev. C **86**, 057305 (2012).

[44] M. Wang, W. J. Sun, B. H. Sun, J. Li, L. H. Zhu, Y. Zheng, G. L. Zhang, L. C. He, W. W. Qu *et al.*, Eur. Phys. J. A **56**, 31 (2020).

[45] S. J. Zhu, J. H. Hamilton, A. V. Ramayya, J. K. Hwang, J. O. Rasmussen, Y. X. Luo, K. Li, J. G. Wang, X. L. Che *et al.*, Chin. Phys. C **33**, 256 (2009).

[46] Y. X. Luo, S. J. Zhu, J. H. Hamilton, A. V. Ramayya, C. Goodin, K. J. Li, X. L. Che, J. K. Hwang, I. Y. Lee *et al.*, Int. J. Mod. Phys. E **18**, 1697 (2009).

[47] I. Kuti, Q. B. Chen, J. Timar, D. Sohler, S. Q. Zhang, Z. H. Zhang, P. W. Zhao, J. Meng, K. Starosta *et al.*, Phys. Rev. Lett. **113**, 032501 (2014).

[48] J. A. Alcántara-Núñez, J. R. B. Oliveira, E. W. Cybulska, N. H. Medina, M. N. Rao, R. V. Ribas, M. A. Rizzutto, W. A. Seale, F. Falla-Sotelo *et al.*, Phys. Rev. C **69**, 024317 (2004).

[49] J. Timár, P. Joshi, K. Starosta, V. I. Dimitrov, D. B. Fossan, J. Molnar, D. Sohler, R. Wadsworth, A. Algora *et al.*, Phys. Lett. B **827**, 137006 (2022).

[50] D. Tonev, M. S. Yavahchova, N. Goutev, G. de Angelis, P. Petkov, R. K. Bhowmik, R. P. Singh, S. Muralithar, N. Madhavan *et al.*, Phys. Rev. Lett. **112**, 052501 (2014).

[51] P. Joshi, D. G. Jenkins, P. M. Raddon, A. J. Simons, R. Wadsworth, A. R. Wilkinson, D. B. Fossan, T. Koike, K. Starosta *et al.*, Phys. Lett. B **595**, 135 (2004).

[52] J. Timár, T. Koike, N. Pietralla, G. Rainovski, D. Sohler, T. Ahn, G. Berek, A. Costin, K. Dusling *et al.*, Phys. Rev. C **76**, 024307 (2007).

[53] C. Y. He, B. Zhang, L. H. Zhu, X. G. Wu, H. B. Sun, Y. Zheng, B. B. Yu, L. L. Wang, G. S. Li *et al.*, Plasma Sci. Technol. **14**, 518 (2012).

[54] E. O. Lieder, R. M. Lieder, R. A. Bark, Q. B. Chen, S. Q. Zhang, J. Meng, E. A. Lawrie, J. J. Lawrie, S. P. Bvumbi *et al.*, Phys. Rev. Lett. **112**, 202502 (2014).

[55] K. Y. Ma, H. Wang, H. N. Pan, J. B. Lu, Y. J. Ma, D. Yang, Q. Y. Yang, X. Guan, J. Q. Wang *et al.*, Phys. Rev. C **103**, 024302 (2021).

[56] M. G. Porquet, T. Venkova, P. Petkov, A. Bauchet, I. Deloncle, A. Astier, N. Buforn, J. Duprat, B. J. P. Gall *et al.*, Eur. Phys. J. A **15**, 463 (2002).

[57] S. Roy, N. Rather, P. Datta, S. Chattopadhyay, R. A. Bark, S. Pal, S. Bhattacharya, R. K. Bhowmik, A. Goswami *et al.*, Phys. Lett. B **710**, 587 (2012).

[58] D. R. Zolnowski, H. Yamada, S. E. Cala, A. C. Kahler, and T. T. Sugihara, Phys. Rev. Lett. **41**, 92 (1978).

[59] G. L. Zhang, G. X. Zhang, S. P. Hu, Y. J. Yao, J. B. Xiang, H. Q. Zhang, J. Lubian, J. L. Ferreira, B. Paes *et al.*, Phys. Rev. C **97**, 014611 (2018).

[60] M. F. Guo, G. L. Zhang, P. R. S. Gomes, J. Lubian, and E. Ferioli, Phys. Rev. C **94**, 044605 (2016).

[61] C. L. Guo, G. L. Zhang, S. P. Hu, J. C. Yang, H. Q. Zhang, P. R. S. Gomes, J. Lubian, X. G. Wu, J. Zhong *et al.*, Phys. Rev. C **92**, 014615 (2015).

[62] K. S. Krane, R. M. Steffen, and R. M. Wheeler, At. Data Nucl. Data Tables **11**, 351 (1973).

[63] K. F. Walz, K. Debertin, and H. Schrader, Int. J. Appl. Radiat. Isot. **34**, 1191 (1983).

[64] M. Bogdanovic, S. Koicki, J. Simic, B. Lalovic, D. Breitig, R. Koch, H. A. Baader, O. V. B. Schult, W. R. Kane *et al.*, Fizika (Zagreb) **11**, 157 (1979).

[65] T. W. Elze, T. V. Egidy, H. U. Freund, B. C. Dutta, and W. Kaiser, Z. Phys. **209**, 497 (1968).

[66] C. Liu, S. Y. Wang, B. Qi, D. P. Sun, C. J. Xu, L. Lu, B. Wang, X. C. Shen, M. R. Qin *et al.*, Int. J. Mod. Phys. E **20**, 2351 (2011).

[67] K. R. Pohl, P. H. Regan, J. E. Bush, P. E. Raines, D. P. Balamuth, D. Ward, A. Galindo-Uribarri, V. P. Janzen, S. M. Mullins *et al.*, Phys. Rev. C **53**, 2682 (1996).

[68] F. Dönau, Nucl. Phys. A **471**, 469 (1987).

[69] T. D. MacMahon, G. R. Massoumi, T. Mitsunari, M. Thein, O. Chalhoub, D. Breitig, H. A. Baader, U. Heim, H. R. Koch *et al.*, J. Phys. G **11**, 1231 (1985).

[70] S. Q. Zhang, B. Qi, S. Y. Wang, and J. Meng, Phys. Rev. C **75**, 044307 (2007).

[71] S. Y. Wang, S. Q. Zhang, B. Qi, J. Peng, J. M. Yao, and J. Meng, Phys. Rev. C **77**, 034314 (2008).

[72] B. Qi, S. Q. Zhang, J. Meng, S. Y. Wang, and S. Frauendorf, Phys. Lett. B **675**, 175 (2009).

[73] B. Qi, S. Q. Zhang, S. Y. Wang, J. Meng, and T. Koike, Phys. Rev. C **83**, 034303 (2011).

[74] H. Jia, B. Qi, C. Liu, and S. Y. Wang, J. Phys. G: Nucl. Part. Phys. **46**, 035102 (2019).

[75] C. Liu, S. Y. Wang, R. A. Bark, S. Q. Zhang, J. Meng, B. Qi, P. Jones, S. M. Wyngaardt, J. Zhao *et al.*, Phys. Rev. Lett. **116**, 112501 (2016).

[76] J. Sethi, R. Palit, J. J. Carroll, S. Karamian, S. Saha, S. Biswas, Z. Naik, T. Trivedi, M. S. Litz *et al.*, J. Phys. G: Nucl. Part. Phys. **43**, 015103 (2016).

[77] C. Liu, S. Y. Wang, B. Qi, D. P. Sun, S. Wang, C. J. Xu, L. Liu, P. Zhang, Z. Q. Li *et al.*, Phys. Rev. C **88**, 037301 (2013).

[78] Y. Zheng, Strange rotation in ^{106}Ag and ^{126}I: chiral rotation, magnetic rotation and signature inversion, Doctoral dissertation, China Institute of Atomic Energy, 2012 (unpublished), p. 73.

[79] D. Jerrestam, W. Klamra, J. Gizon, F. Liden, L. Hildingsson, J. Kownacki, Th. Lindblad, and J. Nyberg, Nucl. Phys. A **577**, 786 (1994).

[80] P. Datta, S. Roy, S. Pal, S. Chattopadhyay, S. Bhattacharya, A. Goswami, M. SahaSarkar, J. A. Sheikh, Y. Sun, P. V. Madhusudhana Rao, R. K. Bhowmik, R. Kumar, N. Madhavan, S. Muralithar, R. P. Singh, H. C. Jain, P.K. Joshi, and Amita, Phys. Rev. C **78**, 021306(R) (2008).

[81] P. Agarwal, S. Kumar, S. Singh, R. K. Sinha, A. Dhal, S. Muralithar, R. P. Singh, N. Madhavan, R. Kumar *et al.*, Phys. Rev. C **76**, 024321 (2007).

[82] G. B. Hagemann and I. Hamamoto, Phys. Rev. C **40**, 2862 (1989).

[83] R. Bengtsson, H. Frisk, F. R. May, and J. A. Pinston, Nucl. Phys. A **415**, 189 (1984).

[84] Y. Liu, J. Lu, Y. Ma, S. Zhou, and H. Zheng, Phys. Rev. C **54**, 719 (1996).

[85] D. J. Hartley, L. L. Riedinger, M. Danchev, W. Reviol, O. Zeidan, J. Y. Zhang, A. Galindo-Uribarri, C. J. Gross, C. Baktash *et al.*, Phys. Rev. C **65**, 044329 (2002).